

# Rotary-Wing Relevant Compressor Aero Research and Technology Development Activities at Glenn Research Center

Gerard E. Welch, Michael D. Hathaway, Gary J. Skoch  
Aerospace Engineers  
U. S. Army Research Laboratory, Vehicle Technology Directorate  
Cleveland, Ohio 44135

[Gerard.Welch@us.army.mil](mailto:Gerard.Welch@us.army.mil), [Michael.Hathaway@us.army.mil](mailto:Michael.Hathaway@us.army.mil), [Gary.Skoch@us.army.mil](mailto:Gary.Skoch@us.army.mil)

Christopher A. Snyder  
Aerospace Engineer  
NASA John H. Glenn Research Center at Lewis Field  
Cleveland, Ohio 44135  
[Christopher.A.Snyder@nasa.gov](mailto:Christopher.A.Snyder@nasa.gov)

## ABSTRACT

Technical challenges of compressors for future rotorcraft engines are driven by engine-level and component-level requirements. Cycle analyses are used to highlight the engine-level challenges for 3000, 7500, and 12000 SHP-class engines, which include retention of performance and stability margin at low corrected flows, and matching compressor type, axial-flow or centrifugal, to the low corrected flows and high temperatures in the aft stages. At the component level: power-to-weight and efficiency requirements impel designs with lower inherent aerodynamic stability margin; and, optimum engine overall pressure ratios lead to small blade heights and the associated challenges of scale, particularly increased clearance-to-span ratios. The technical challenges associated with the aerodynamics of low corrected flows and stability management impel the compressor aero research and development efforts reviewed herein. These activities include development of simple models for clearance sensitivities to improve cycle calculations, full-annulus, unsteady Navier-Stokes simulations used to elucidate stall, its inception, and the physics of stall control by discrete tip-injection, development of an actuator-duct-based model for rapid simulation of nonaxisymmetric flow fields (*e.g.*, due inlet circumferential distortion), advanced centrifugal compressor stage development and experimentation, and application of stall control in a T700 engine.

## NOTATION

AATE	=	Advanced Affordable Turbine Engine
b	=	impeller exit blade span
c	=	chord
h	=	blade height (span)
g	=	staggered gap
JHL	=	Joint Heavy Lift
LCTR	=	Large Civil Tilt-Rotor
$\dot{m}$ , $\dot{m}_c$	=	mass flow rate, corrected mass flow rate
OPR	=	overall pressure ratio
SHP	=	shaft horsepower
SFC	=	specific fuel consumption
SP	=	specific power
$T_3$	=	compressor discharge temperature
$T_4$	=	turbine entry temperature
$\delta^*$	=	aerodynamic blockage
$\epsilon$	=	clearance ( <i>e.g.</i> , in mils)
$\eta$	=	efficiency
$\psi$	=	pressure rise coefficient
$\phi$	=	flow coefficient

## INTRODUCTION

An overview of rotorcraft-relevant compressor research and technology development activities underway at Glenn Research Center is provided herein. The research activities are sponsored by the NASA Subsonic Rotary Wing (SRW) project and are intended to address key aerodynamic challenges associated with the compressors of the type used in advanced turboshaft engines of the 3000 (DoD AATE<sup>1</sup>), 7500 (NASA LCTR<sup>2,3</sup>), and 12000 (DoD JHL, cf. Ref. 4) SHP-class. A particular objective of the described research is to support technology development of the 7500 SHP-class engines for the NASA LCTR mission.

The principal challenge posed by the LCTR mission is the requirement to reduce the main rotor speed from 650 ft/s at ground take-off to 350 ft/s at Mach 0.5 cruise (Acree *et al.*<sup>3</sup>) Although the rotor speed is reduced by approximately 50%, the specific power levels (SHP/lb<sub>m</sub>/s) at the take-off and cruise points are essentially the same. This requirement for wide variability in rotor speed represents a significant departure from the nearly constant-speed operation of conventional rotorcraft. The required variability impels research and technology efforts related to i.) variable-speed transmission and/or ii.) variable-speed power-turbine output. While the power-turbine shaft speed can vary by a factor of two in the latter approach, preliminary cycle analyses of the LCTR mission indicate that the gas generator components

(compressor and HPT) operate at approximately constant corrected conditions and no additional operability requirements are imposed on the compression system (Snyder and Thurman<sup>5</sup>).

The technical challenges for the compressors are related to aerodynamics of low corrected flows ( $\dot{m}_c \propto \dot{m}\sqrt{T}/p$ ) in aft stages, strength-of-materials and cooling limitations at elevated compressor discharge temperatures, and stability. These challenges are discussed in the first part of the paper. This is followed by an overview of on-going modeling, component testing, and engine testing activities intended to address these challenges.

## COMPRESSOR TECHNOLOGY CHALLENGES

The technical challenges for the compressors are driven by engine system and component level requirements.

### Engine-Level Challenges

At the engine level, the high power-to-weight and fuel efficiency requirements of rotorcraft engines push overall pressure ratios (OPRs) to increasingly higher levels. Example curves for SFC and specific power (SP) as functions of OPR for the 3000, 7500, and 12000 SHP engine classes are shown in Fig. 1. These results were obtained using the Numerical Propulsion System Simulation (NPSS) code (Jones<sup>6</sup>), for the fixed turbine entry temperatures indicated in Fig. 1, specified technology correlations for turbine cooling effectiveness as a function of cooling flow (Gauntner<sup>7</sup>), and compressor polytropic efficiency as a function of compressor exit-corrected flow (Fig. 2). The influence of the higher temperature cooling air and degradation of compressor efficiency in the aft-stages at increased OPR, leads to the optima in OPR, in terms of SFC minimization, as shown in Fig. 1a.

The high engine OPRs introduce technical challenges associated with the aerodynamics of low corrected flows and blade heights (Figs. 3a and 3b) and high compressor discharge temperatures ( $T_3$ , Fig. 4). In engines of a fixed SHP level, these challenges only worsen as  $T_4$  (and hence SP) is increased, leading to engines of lower mass flow rate and higher optimum OPR. The challenges associated with low corrected flows and high  $T_3$  are highlighted in the following sections, engine by engine.

### 3000 SHP-class engines

At the 3000 SHP (AATE) level with physical flow rates of 11-13 lb<sub>m</sub>/s, aft stage exit-corrected flow rates ( $\dot{m}_{c,3}$ ) can be less than 0.75 lb<sub>m</sub>/s (see Fig. 3a). At these flow sizes and associated small blading (Fig. 3b), the centrifugal compressor overtakes the axial compressor in terms of efficiency, as shown notionally in Fig. 2a, compactness, and weight. The cross-over point in terms of exit-corrected flow (e.g., 1.5 lb<sub>m</sub>/s), while dependent weakly on aero technology levels and engine size, is the point at which the aerodynamics of the axial stages is degrading rapidly—due to the effects of relatively large clearance-to-span, blade-tolerances, and relative boundary-layer (aero-blockage) fractions. An important technical challenge in the 3000 SHP engine size is related, in part, to retaining high efficiency in compact, highly loaded axial and centrifugal compressors with low corrected flows. Overcoming this challenge impels research related to management of loss associated with large impeller-tip/shroud clearance-to-exit-span ratios, relative fillets, and blade thickness (cf. scaling study of Skoch and Moore<sup>8</sup>). Considering the stress levels sustained by aft stage centrifugals, engine pressure ratio—or specifically the associated compressor discharge temperatures,  $T_3$ —may well be limited by the strength of impeller materials required to meet life (as suggested in Fig. 4).

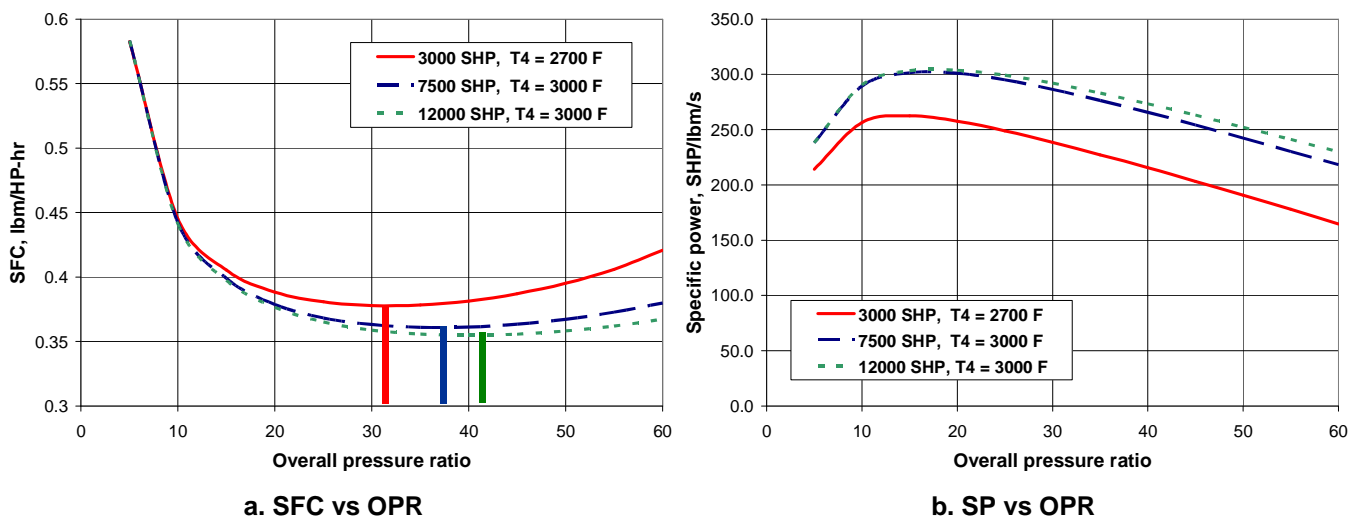
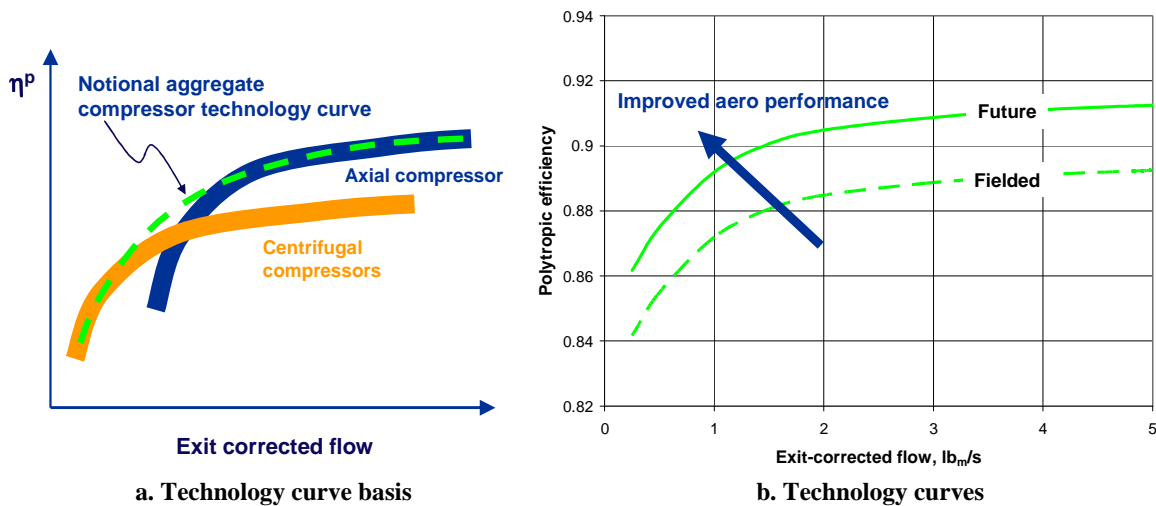


Figure 1. Engine cycle calculation results, showing a.) SFC and b.) specific power as a function of OPR for the 3000, 7500, and 12000 SHP-class engines.



**Figure 2. Notional compressor technology curves showing a.) design-point polytropic efficiency as function of exit-corrected flow for centrifugal and axial-flow compressor stages, and representative aggregate performance curve (green/dashed) used in cycle analyses herein; and, b.) projected improvements in notional aggregate compressor efficiency levels to be achieved by aerodynamic improvements.**

### 7500 SHP-class engines

In the 7500 SHP-class engines, the physical weight flows (e.g., 25 lb<sub>m</sub>/s) and optimum OPR (e.g., 37:1) lead to compressor exit-corrected flows near unity (see Fig. 3a). This power class engine may prove particularly challenging to compressor aero. At this corrected flow, centrifugal stages would be preferable to axial stages (Fig 2a); however, the  $T_{3s}$  associated with these OPRs might prove incompatible with the high stress levels of centrifugal impellers, and axial stages might need be used, even at the relatively low aft-stage corrected flows (< 1 lb<sub>m</sub>/s). The technical challenges in the aft axial stages are thus related to maintaining high efficiency with small blade heights (< 0.5 in.). This technical challenge is a subject of research in a companion NASA project (Subsonic Fixed Wing) related to the aerodynamics of low-corrected flows in aft axial stages of high OPR ultra-

high bypass ratio engines. The blade heights of these engines are envisaged comparable to those shown for the 7500 SHP-class engine (Fig. 3b). As suggested by Fig. 4, if/when impeller/backplate materials with increased strength at temperature are employed, use of a centrifugal compressor to replace aft axial stages may be warranted in this engine class.

### 12000 SHP-class engines

The 12000 SHP-class engines (JHL) will have relatively high physical mass flow rates (e.g., 45 lb<sub>m</sub>/s) at high OPRs (e.g., 42:1) leading to exit-corrected flows of about 1.5 lb<sub>m</sub>/s. At these corrected flows and high temperatures, an all-axial compressor would be expected. The technical challenges are again related to the aerodynamics of low-corrected flow in axial aft-stages.

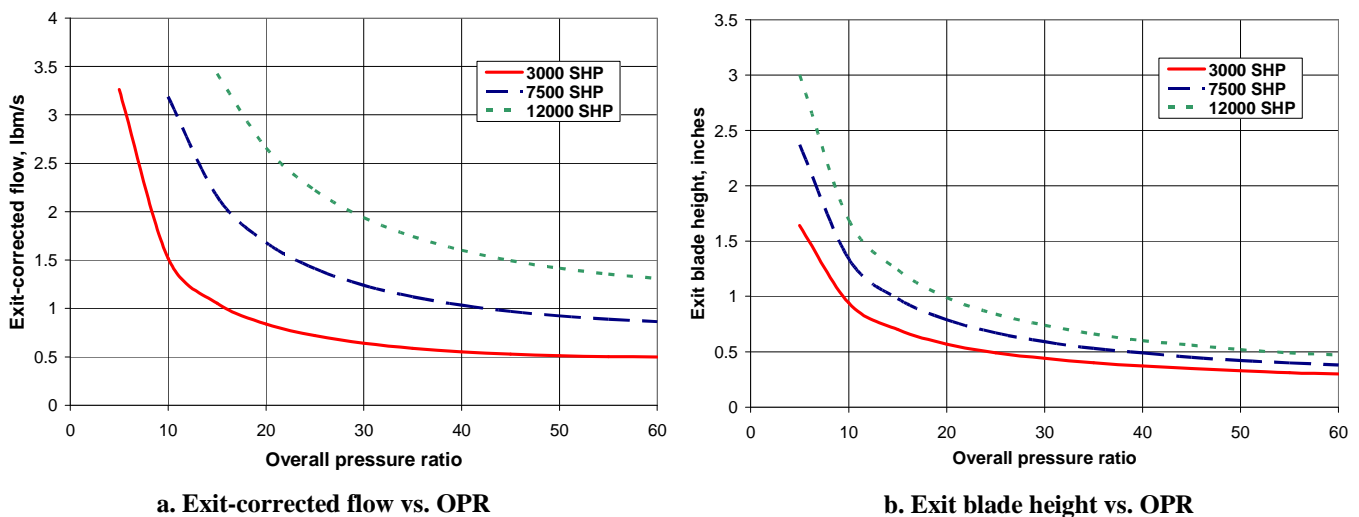


**Figure 3. Exit-corrected flow in example 3000, 7500, and 12000 SHP engines as a function of OPR.**

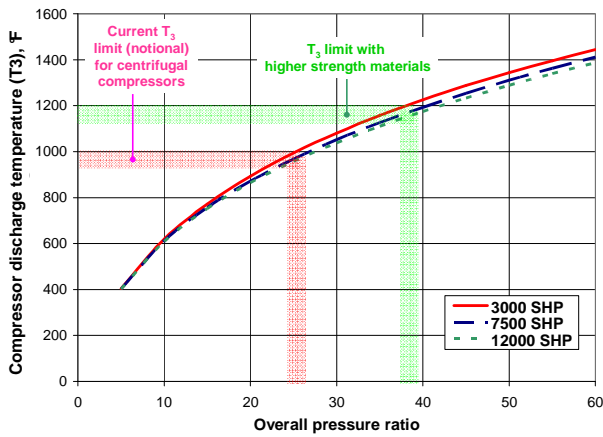
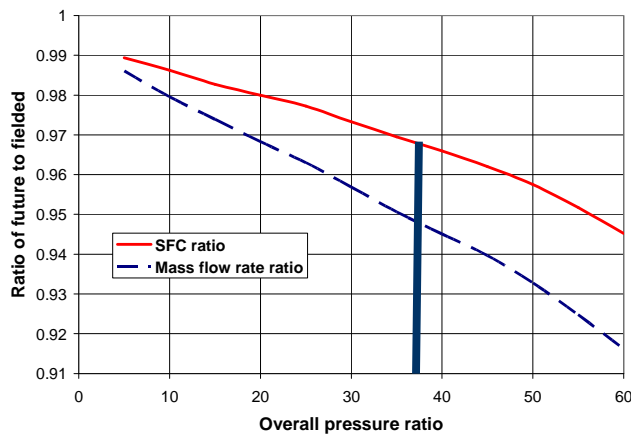


**Figure 4. Compressor discharge temperature ( $T_3$ ) in example 3000, 7500, and 12000 SHP engines as a function of OPR, showing opening of OPR-space accessible by higher temperature materials capabilities.**

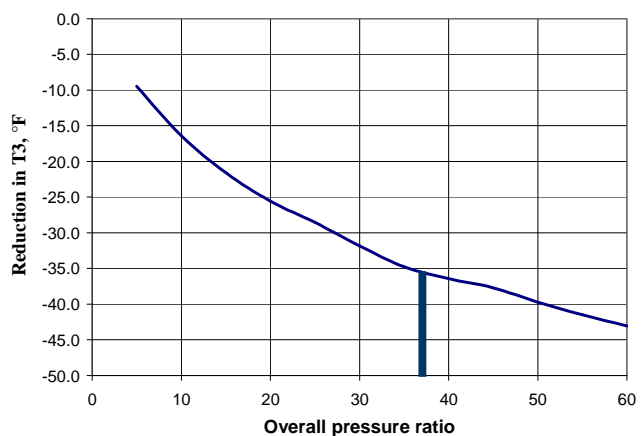
### Component Level Challenges

The impact of compressor polytropic efficiency on LCTR-class (7500 SHP) engine efficiency (fuel consumption), size (weight), and available turbine cooling temperatures ( $T_3$ ) is shown in Fig. 5. Considering an example OPR of 37:1 (see Fig. 1a), a two point increase in polytropic efficiency, from “fielded” to “future” technology levels (Fig. 2b *viz.* Fig. 3a), leads to a 3% reduction in fuel consumption (Fig. 5a) and a 5% reduction in engine mass flow rate (Fig. 5a). Additionally, the same technology improvement would lead to 35 °F cooler compressor discharge temperature at the 37:1 OPR (Fig. 5b). These benefits highlight the importance of addressing technical challenges associated with improving component efficiency by managing blade row losses (3-D aero designs), clearances, and leakages, and insuring stage matching so that blade rows operate as per design-intent.

Power-to-weight requirements force high aerodynamic loading levels associated with compactness (low weight)



**a. SFC and mass flow rate ratios**



**b. Reduction in compressor discharge temperature**

**Figure 5. Impact of two-point increase in compressor polytropic efficiency (cf. Fig. 2b) from fielded to future engine in terms of a.) ratios of specific fuel consumption and mass flow rate; and, b.) compressor discharge temperature,  $T_3$ .**

requirements. Concurrently, the aero-loading levels must be tempered by the component efficiency and stall margin required to meet engine efficiency and operability. These factors push designers to stage designs with lower inherent aerodynamic stability margin—a design trade which may be acceptable in advanced engines if active stability management methodologies are realizable (cf. Larosiere *et al.*<sup>9</sup>). The technical challenges then associated with highly efficient, high power density compressor components involve development of efficient and reliable stability management, or stall control, technologies.

As the corrected flows decrease with increasing OPR (Fig. 3a.) and the aft-stage blade heights are reduced (Fig. 3b): The aft axial stages are pushed to higher hub-to-tip ratios in general, the blade counts increase, and/or the aspect ratios decrease; the minimum blade thicknesses and fillets at the small sizes and high temperatures may well be set by material/strength requirements or machining tolerances rather than aero considerations; and, the impact of endwall and clearance flows takes on relatively stronger importance. The management of endwall aerodynamic blockage levels, in particular, becomes increasingly challenging as the relative clearances ( $\epsilon/h$ ) increase.

### COMPRESSOR RESEARCH ACTIVITIES

Specific computational and experimental research activities described below are intended to address the technical challenges associated with the aerodynamics of aft stages with low corrected flows and compressor stability. With regards to compatibility with low corrected flows, a rudimentary clearance flow modeling effort is first described, followed by a description of centrifugal compressor research activities in the NASA Small Engine Components Test Facility. With regards to stability, three activities are then described: T700 engine/stall-control testing and supporting unsteady Navier-Stokes computations; and, the development of a new actuator-duct based nonaxisymmetric throughflow model.

## Modeling for Improved Engine Cycle Calculations

The reduction in aerodynamic performance at low corrected flows must be accounted for in the engine performance calculations (as was approximated herein through the compressor technology curve, Fig. 2b). The impact of rotor/impeller tip clearance ( $\varepsilon/h$  or  $\varepsilon/b$ ), in particular, is critical given its impact on both compressor performance and stability. Typical clearance sensitivities for pressure ratio, efficiency, flow, flow range, and stability are documented in the literature, and are shown qualitatively in Fig. 6a. As the clearance-to-chord (or span,  $\varepsilon/h$  or  $\varepsilon/b$ ) increases, stage efficiency, stability margin, pressure ratio, and flow range generally decrease. Cumpsty<sup>10</sup> has summarized key references for clearance sensitivities for both centrifugal and axial compressors. For example, Wisler<sup>11</sup> has reported for a low-speed four-stage axial compressor that an increase in clearance-to-chord from 1.6 to 3.4 percent led to a 1.5% reduction in efficiency, and 11% reduction in flow range, and a 9.7 percent reduction in peak pressure rise, while Freeman<sup>12</sup> found a 1.4% decrease in efficiency for a one point change in clearance to chord in a high-speed multistage compressor. Similarly, in centrifugal compressors, roughly 0.25% in efficiency is sacrificed for every 1% clearance to exducer-span ( $\varepsilon/b$ , cf. Skoch and Moore<sup>8</sup>). In terms of engine cycle modeling, the clearance sensitivities are of interest for both design-point performance estimates and for transients (*i.e.*, case and rotor differential cooling effects). In terms of design-point estimates, as OPR increases the ratio of an acceptable running clearance (*e.g.*, 15 mils) to the aft-stage blade height (see Fig. 3b) increases strongly. For example, if the ratio of a clearance to chord of an LCTR (7500 SHP) engine at 20:1 (and  $\dot{m}_{c,ex} \approx 1.7 \text{ lb}_m/\text{s}$ ) was  $\varepsilon/c \approx 2\%$ , then using Fig. 3b the same aspect ratio blading at 40:1 ( $\dot{m}_{c,ex} \approx 1$ ) would have  $\varepsilon/c \approx 3\%$ . In light of the sensitivities cited for the axial compressors above, the loss in aft-stage efficiency attributable to reduced relative clearances alone for this increase in OPR would be expected to be 0.8 to 1 point (cf. Fig. 2b).

A simplified model to account for the impact of increased relative clearances is under development using documented sensitivities of this kind. The compressor characteristic ( $\psi - \phi$  and  $\eta - \phi$ ) at a given corrected speed are determined (see Robbins and Dugan<sup>13</sup>) from known (or design-intent) performance characteristics and clearance ( $\varepsilon/c$ ). Herein, the pressure rise characteristic is modeled as  $\psi/\psi_{\max} = 1 - \mathcal{R} \cdot \left(\frac{\phi}{\phi_{\min}} - 1\right)^2$ , where  $\psi_{\max}$  is the pressure coefficient at stall (maximum),  $\phi_{\min}$  is the stalling flow coefficient, and  $\mathcal{R} = -\frac{1}{2} \frac{\partial^2 \psi}{\partial \phi^2} \cdot \frac{\phi_{\min}^2}{\psi_{\max}}$  sets the curvature of the characteristic. For a given clearance, the stalling pressure ratio as a function of percent  $\varepsilon/c$  is determined from the correlation of Smith,<sup>14</sup> which documents a 4.6% peak

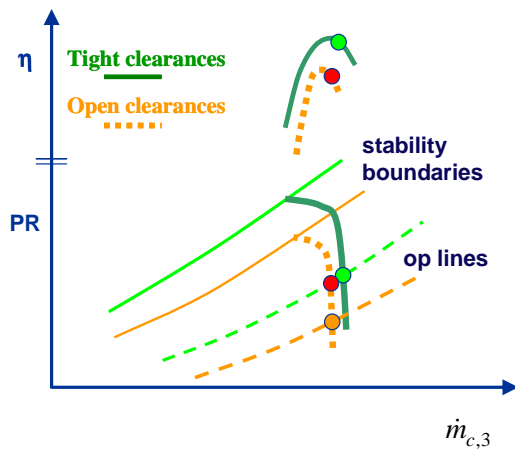
pressure loss for each 1% clearance-to-chord. The aerodynamic blockage ( $\delta^*$ ) at this stability boundary is estimated using the correlation of Koch and Smith<sup>15</sup> and is a function of the clearance to stagger-gap ratio ( $\varepsilon/g$ ). The percent of span corresponding to the aerodynamic blockage fraction ( $\delta^*/h$ ) is assumed to do no work and the stalling flow rate is back calculated using the known compressor characteristic and the stalling pressure ratio from the Smith correlation.

The model is in its inception and is certain to undergo refinement during its implementation and validation. Preliminary results in Fig. 6b indicate the calculated impact of clearance variations on the performance characteristics at 50% and 100% corrected speeds. The clearance strongly reduces the stability margin and maximum pressure rise capability of the compressor. The efficiency is reduced concomitantly, according to the sensitivities described above (*e.g.*, 1.4% decrease in  $\eta$  for each 1% increase in clearance-to-chord).

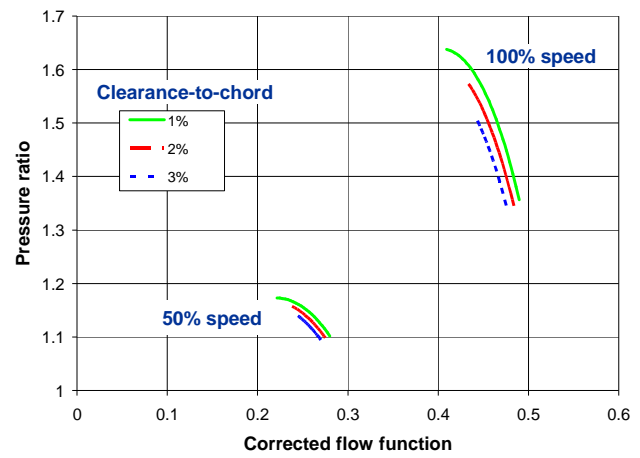
## Experiments in the Small Engine Components Test Facility

Experimental research on both axial and centrifugal compressor aerodynamics has been conducted in the NASA Small Engine Components Test Facility (SECTF, see Brokopp and Gronski<sup>16</sup>) over the past twenty-five years. The SECTF (Fig. 7a) is ideally suited for testing rotorcraft-relevant single and multistage compressors. A 6000-hp variable frequency drive motor and gearbox is used to drive the research article at speeds up to 60,000 rpm. The throttle valve and exhaust sprayer cooler are rated for operation at pressure ratios up to 30:1. Inlet air pressure can be varied from 2 to 50 psia and temperature from ambient down to -50 °F. Maximum flow capacity, dependent on inlet conditions, is in the range 40 to 65  $\text{lb}_m/\text{s}$ . The rig, as configured currently, can accommodate compressors up to 20 in. diameter.

Skoch and Moore carried out a centrifugal compressor scaling study during the late '80s which documented efficiency sensitivities to variations in clearance ( $\varepsilon/b$ ), fillet size, and Reynolds number.<sup>8</sup> Laser Doppler velocimetry (LDV) was subsequently used to characterize the impeller discharge flow and vane-island diffuser flow in a series of experiments by Skoch *et al.*<sup>17</sup> and Wernet *et al.*<sup>18</sup> The laser anemometry efforts provided valuable flow field data sets for code validation (see, for example, Larosiliere *et al.*<sup>19</sup>), and were followed by a series of stall control experiments (discussed below). In addition to small (2.5  $\text{lb}_m/\text{s}$ ) and large (10  $\text{lb}_m/\text{s}$ ) centrifugal compressors, a  $\dot{m}_{c,ex} = 10.5 \text{ lb}_m/\text{s}$  ( $\dot{m}_{c,ex} \approx 2.75 \text{ lb}_m/\text{s}$ ), 2.5-stage with 5:1 design-point pressure ratio was tested in the SECTF facility as well (Adamczyk *et al.*).<sup>20</sup>



a. Impact of clearance at constant speed



b. Model results

**Figure 6. Impact of increased clearances on compressor performance, showing a.) expected impact on pressure rise, efficiency, stall margin, flow, and flow range, and b.) modeled impact of clearance on performance curves intended for use in cycle calculations.**

The SECTF went into standby in 2003. Under the current NASA Subsonic Rotary Wing project, the test cell has been restored to an operational state. This investment is to enable in-house research of advanced centrifugal compressors with open geometry, to provide a facility for research formulated with industry and academia, and for DoD/industry collaboration. The SECTF is currently being used to re-baseline the 4:1 CC3 compressor stage (Fig. 7b) comprising the impeller, vane-island diffuser, and 90 degree turning duct (no deswirl vanes).<sup>17</sup> The 10 lb<sub>m</sub>/s CC3 compressor is a scaled-up version of a 3.6 lb<sub>m</sub>/s stage that facilitates detailed flow anemometry. Following baseline performance measurements, the 50 mil variable clearance capability of SECTF will be exercised to re-establish clearance sensitivities for performance and range. Current

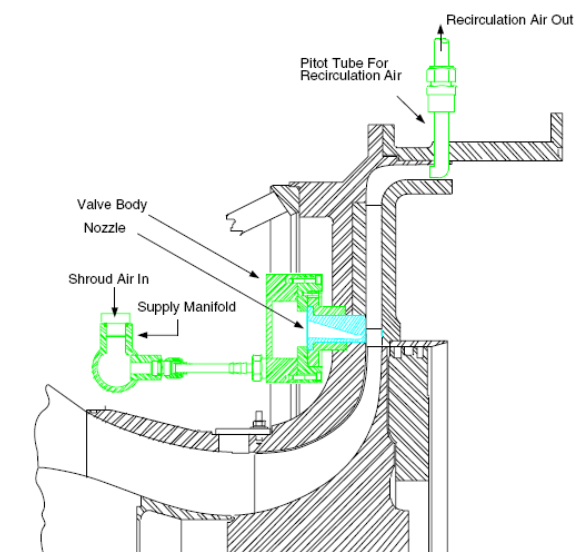
entry plans also include acquisition of  $r-\theta$  surveys downstream of the vane-island diffuser—a first in CC3—and radial surveys of high-response total-pressure in the vaneless space between the impeller and diffuser.

#### NASA Research Announcement Contract on Advanced Centrifugal Compressors

A 2007 NASA Research Announcement (NRA) solicitation included requests for proposals to support advanced centrifugal compressor research and development with an aim to improve design methodologies and component performance levels for future rotorcraft applications. The objectives of the three-year activity were to include the following:



a. Small Engine Component Test Facility



b. Cross-section of CC3 compressor stage

**Figure 7. a.) photo of SECTF and b.) CC3 cross-section showing shroud stall control injection scheme.**

- identify and prioritize key knowledge gaps, and outline experimental testing needed to advance the state-of-the-art of rotorcraft-relevant (Table 1) centrifugal compressor technology;
- determine research measurements required for tool validation and for needed insight into salient flow physics;
- design, fabricate, install and collaboratively test a advanced, rotorcraft-relevant, centrifugal compressor research test article in the SECTF to obtain detailed aerodynamic and aeromechanical measurements; and,
- acquire high-quality research measurements needed to clarify flow physics phenomena and to establish detailed data sets for development and validation of new methods.

A three-year NRA contract was awarded to United Technologies Research Center (UTRC) in late 2008. A research centrifugal compressor stage—impeller, diffuser, turning duct, and deswirl vanes—which has key attributes (cf. Table 1) appropriate to state-of-the-art rotorcraft engines, is to be designed, built, and tested in the SECTF as a follow on to current CC3 experimentation. Table 1 reflects a highly aggressive compressor design in terms of the combined efficiency, work factor, stall margin, and compactness (weight) requirements. Like CC3,<sup>17</sup> the new test article will be scaled-up to the 10 lb<sub>m</sub>/s flow size so as to accommodate detailed flow field measurements. The scaling will maintain tolerances, relative fillet sizes, and blade thickness to insure aerodynamic similitude with a 2.5 to 3 lb<sub>m</sub>/s rotorcraft-relevant application compressor. The centrifugal stage is scheduled for delivery and installation during FY10 and check-out testing and baselining at the end of FY11; thereafter, the test article is intended to be used by the government, industry, and academia to acquire key consensus data sets.

**Table 1 – NRA solicitation – application compressor design-point characteristics.**

Metric	Value or Range
Stage pressure ratio	4.5 < PR < 6
Inlet corrected flow	$2.5 \leq \dot{m}_{c,in} \leq 3$ lb <sub>m</sub> /s
Stage-exit corrected flow	$0.7 \leq \dot{m}_{c,ex} \leq 0.8$ lb <sub>m</sub> /s
Work factor	$0.60 \leq \Delta H_o / U_{ip}^2 \leq 0.75$
Polytropic stage efficiency	$\geq 0.88$
T3 capability	950 < T (°F) < 1000
Max flow path diameter to impeller tip diameter	$r_{max} / r_{ip} \leq 1.45$
Design stability margin	25%

## Stall Control Activities

The Active Stall Control Engine Demonstration (ASCED) project was initially funded by the U.S. Army Research Laboratory (ARL) and was completed with augmentation funding from the Subsonic Rotary Wing Project of the NASA Fundamental Aeronautics program. The project had both engine testing (experimental) and computational modeling aspects (next section). The objective of the project was to demonstrate stall control technologies, which had been developed earlier in NASA axial and centrifugal compressor component experiments, in an engine. The intent was to understand the impact of integration and operation in the engine environment on achieved flow range extension. In the following sections, the key findings from the earlier components experiments are first provided, followed by overviews of on-going experimental and computational stall control activities.

### Earlier NASA component experiments

Suder *et al.*<sup>21</sup> demonstrated flow range and stability improvements in transonic, single-stage, axial-flow compressors and fans using steady-state injection through discrete injectors upstream of the compressor rotor. The discrete injectors were distributed circumferentially about the compressor case and were operated in choke. The emitted jets effectively unload the rotor tip regions and in this way reduce the aerodynamic blockage levels at the case that lead to stall. Suder *et al.* (2001)<sup>21</sup> determined that the arrangement of the injectors in terms of their relative circumferential position was less important to flow range extension than were the number of injectors and the axial velocity of each jet. A Coanda injector, suitable for integration between blade rows was demonstrated as well and later assessed in a high-performance multistage compressor (Strazisar *et al.*).<sup>22</sup>

Skoch extended the steady injection work just described to centrifugal compressors<sup>23,24</sup> and demonstrated stability margin enhancement (+1.7%) using injectors that directed air-jets along the shroud surface in the vaneless region between the impeller and vaned diffuser (Fig. 7b). Similar hub-side injection in the vaneless region was found to be less effective. In addition to steady shroud-side air injection, Skoch found that tubes protruding into the vaneless region through the shroud surface improved stability margin by 4.4%. Both the injectors and stall-control-tubes have an associated pressure ratio penalty of approximately 1% in the centrifugal compressor, depending upon the injection flow rate or control-tube immersion.

### T700 engine experiments

The stall control technologies described above were subsequently applied in a T700 engine tests. The T700 turboshaft engine was selected for the engine demonstration of stall control due to its important role in powering the Army helicopter fleet. The compressor of the T700 engine has five and a half axial stages, the first three of which have variable inlet-guide-vanes/stators, followed by a single-stage

centrifugal. Experiments were carried out in the NASA Engine Components Research Laboratory (ECRL, Fig. 8), and involved stall control in both the axial and centrifugal stages. The axial and centrifugal compressors could be throttled independently by preferential back-pressuring using externally controllable inflow of high-pressure air.

Coanda injectors of the type demonstrated by Strazisar *et al.*<sup>22</sup> were installed ahead of Rotors 1, 2 and 5 of the axial compressor. The injection air was supplied from either an external high pressure source with temperature control or by recirculation from within the engine. Injectors at the Rotor 1 and 2 locations were supplied by air extracted downstream of the last axial stage, while Rotor 5 injectors were supplied from air extracted downstream of the centrifugal compressor stage. In addition to the air injectors in the axial compressor, retractable, solid, stall control tubes were installed at multiple locations around the circumference in the vaneless space ahead of the centrifugal compressor diffuser.



**Figure 8. Photograph of the NASA Engine Component Research Laboratory with T700 engine and stall control injection air lines installed.**

Example results for tip injection in the axial compressor are shown in Fig. 9 where range extension is indicated for operation at 80% speed. In the upper chart, three of the six available injectors ahead of Rotor 1 were active as the axial compressor was throttled. Tip injection provided a 3.5% increase in flow range, while maintaining stall pressure ratio.

The ECRL test facility provides robust data collection capability. In addition to versatile injector and engine controls, the ARL/NASA T700 engine is heavily instrumented. Total pressures and temperatures are measured upstream and downstream of both the axial and centrifugal compressors. The leading and trailing edge of each axial blade row, rotors and stators are instrumented with steady-state casing static-pressures. High-response pressure measurements are collected upstream of each axial rotor as well. In the near future, a light probe system will be added to measure blade vibration during stall and surge. The diffuser is similarly heavily instrumented with steady-state and high-response pressure instrumentation.

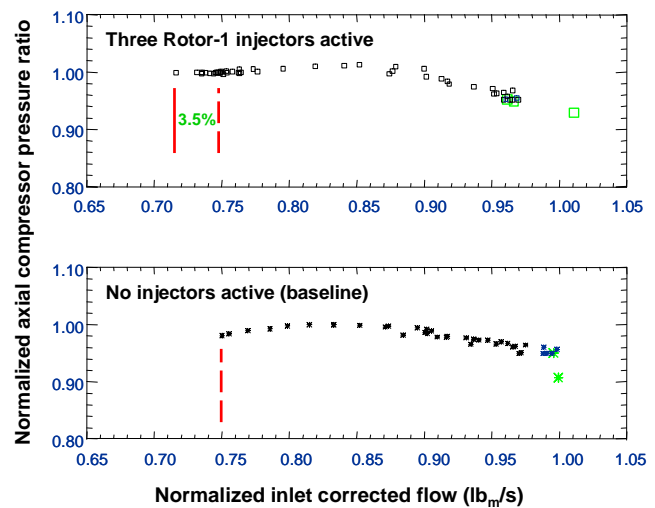


**Figure 9. Demonstrated stall control in five-stage axial compressor in T700 engine at (80%) operating speed, showing flow range extension achieved by injection ahead of Rotor 1.**

#### URANS simulations of stall inception & control

In addition to the T700 engine testing, the ASCED program included a compressor simulation element. Unsteady Reynolds-averaged Navier-Stokes (URANS) equation simulations have been used to elucidate the causal mechanisms and associated flow physics leading to stall—that is, stall inception—and the rotor-passage-level impact of the discrete casing endwall injection used for stall control. The simulations complement component level (see Weigl *et al.*<sup>25</sup>) and engine level (above) experiments aimed at understanding stall inception and were intended to provide guidance in the development and testing of tip injection stall control technology. In this section, a brief review of the simulation activities is provided, including their application to support T700 engine experiments.

Initially steady axisymmetric simulations (Hathaway and Strazisar<sup>26</sup>) with and without casing tip injection modeled, indicated that stall was initiated when the rotor tip section exceeded a critical incidence (or max. diffusion factor), and that injection velocity and number of injectors (specifically circumferential coverage) were key parameters for effective range extension (and cf. Suder *et al.*<sup>21</sup>). Such axisymmetric simulations did not admit the non-engine order, non-axisymmetric spatio-temporal flow field variations associated with stall inception and stall; indeed, modeling stall and its inception requires time- and CPU-intensive 3D, unsteady full-annulus simulations. Full-annulus simulations were thus conducted for both axial-flow and centrifugal compressors with a principal objective to further understand the causal fluid mechanisms of rotating stall (Hathaway *et al.*<sup>27</sup> and Chen *et al.*<sup>28</sup>). Subsequent simulations (Chen *et al.*<sup>29</sup>) of the axial compressor as it was throttled to stall demonstrated the ability to simulate the initiation of flow instabilities and their subsequent growth into a fully developed rotating stall, without introduction of an embryonic disturbance.

The beneficial impact of steady tip injection has been demonstrated in recent simulations in which modeling of the discrete tip injection stall control technology has been included (Chen *et al.*<sup>30</sup>). The analyses have indicated that, without stall control, the initial regions of low or reversed axial velocity (disturbance cells) first develop in the mid-span region of the rotor suction surfaces (Fig. 10a), most likely due to the increased incidence and diffusion factor values for this region as it is throttled beyond the stable operating point. These disturbance cells migrate toward the tip region while moving downstream. They increase in size as they move to the more highly loaded tip region. When tip injection is of sufficient magnitude to stabilize the compressor, the disturbance cells are successively eliminated by the injectors (Fig. 10b). Some disturbance cells were eliminated after passing through only one injector, while others must pass through multiple injectors before being eliminated.

While stall control by tip injection has been demonstrated to extend operation beyond the baseline (non-injection) stability boundary, the achieved stall range extension is limited by the magnitude and circumferential extent of injection and the ability of the lower spans to accommodate the increase stall range capability. As described, the compressor with tip injection is throttled ever deeper beyond the non-injection stall point, the lower spans subsequently exceed their loading capability (high incidence and diffusion factor) resulting in local reverse flow pockets that centrifuge out to the rotor tip coalescing into stall cells, which eventually grow and spill flow ahead of the rotor leading edge, eventually leading to stall (see Fig 11).

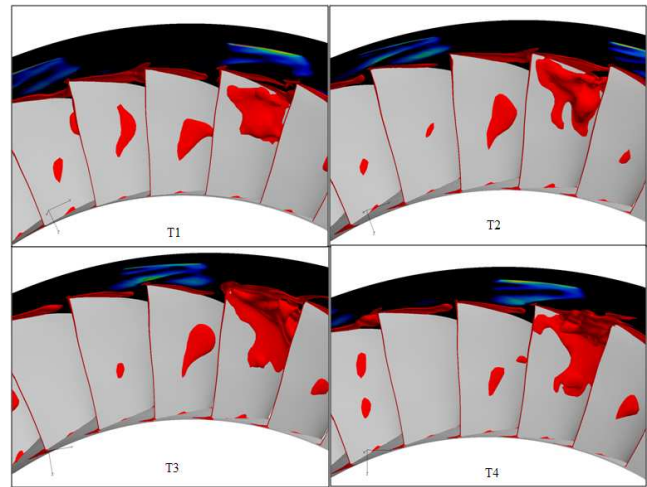
Both steady axisymmetric and unsteady full-annulus simulations of the 5½-stage axial compressor of the T700 engine were conducted in support of the ASCED project (Hathaway *et al.*<sup>27</sup>). Efforts to simulate the centrifugal compressor stage were also initiated with an eye toward simulating the complete T700 axi-centrifugal compression system, both with and without stall control technology. These computationally intensive simulations involved thousands of processors and CPU-months worth of computations to determine the stall boundaries. The investment proved impractical for generic engine simulation in which bleed flows, secondary flows, and variable geometry schedules strongly impact operability. While the URANS simulations continue to serve a role in elucidating the flow physics of stall and its inception, more rapid and less CPU intensive computations are required for rapid simulation of full-annulus, unsteady compressor flow fields.

### Unsteady Actuator-Duct Solver for Nonaxisymmetric Flows

To this end, a more recent effort involves development of a 3-D, unsteady, non-axisymmetric actuator-duct model for rapid simulation of multistage transonic fans/compressors with non-axisymmetric flow fields of low azimuthal wave number. The model is intended for the simulation of the steady and dynamic response of multistage and multi-spool compression systems subjected to generalized inlet circumferential distortions and other nonaxisymmetric effects, including discrete endwall injection.



**a. Radial migration of the disturbance at 0.4 rotor pitch steps per frame in the rotor in stabilized operation beyond baseline stability boundary.**



**b. Disturbance reduction via discrete tip injectors at 0.8 rotor pitch time increments per frame in stabilized operation beyond baseline stability boundary.**

**Figure 10. Pictures of computed instantaneous size and location of local regions of reversed flow (disturbances) in a tip-injection stabilized rotor operating beyond the baseline stability boundary, showing a.) radial transport of disturbances from mid-span to tip region and b.) clean-up of disturbances in tip region by injected flow (Chen *et al.*<sup>30</sup>).**

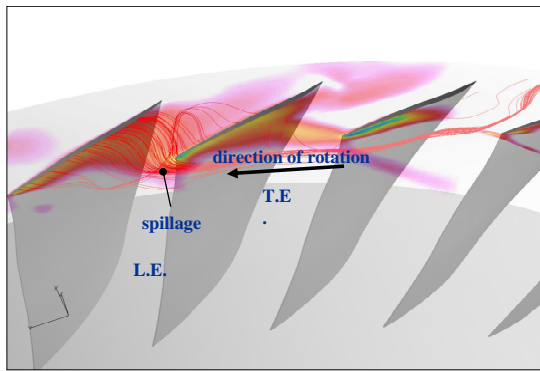
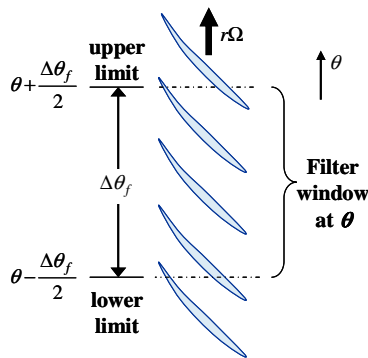
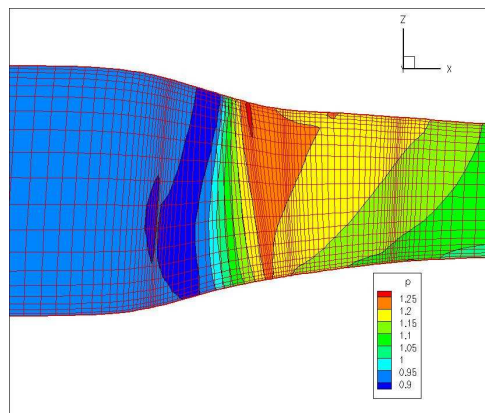


**Figure 11. Computed streaklines of clearance flow during near-stall operation, showing spillage of clearance flow past rotor leading edge (Chen *et al.*<sup>30</sup>).**

The Navier-Stokes equations are low-pass filtered (Fig. 12a) in the circumferential direction, resulting in governing equations which admit only long wavelength circumferential nonuniformities (*e.g.*, wave numbers less than blade count) and which cannot resolve the short wavelength nonuniformities at the blade-passage level (cf. Xu *et al.*<sup>31</sup>). The filtered equations are similar in form to the Navier-Stokes equations, with the addition of body force terms for the blade forces and an additional transport equation for the kinetic energy associated with the shorter (filtered) wavelength distortions. The kinetic energy of the short wavelength distortions is convected by the mean flow, transported by accelerations due to flow work, produced by viscous dissipation and dilatation flow, produced by power (dissipation) due to blade forces, and produced or destroyed by a term which scatters energy to/from the deviation and filtered flow fields. The Harmonic Balance technique (Thomas *et al.*<sup>32</sup>) is used to resolve the circumferential derivative of the  $\theta$ -flux term as in the earlier compressor model for generalized inlet distortions by Welch,<sup>33</sup> resulting in an additional source term that couples  $2N+1$  “throughflow” solutions at equally spaced  $\theta$ -locations, where  $N$  is the maximum wave number (harmonic order) of the solution.



**a. Schematic of low-pass filter**



**b. Computed static pressure contours**

**Figure 12. a.) Schematic showing low-pass filtering at local circumferential position; and, b.) computed contours of static pressure for NASA Rotor 35 at 100% speed, steady-state operation (axisymmetric case).**

The blade forces must be supplied to the computation, and are currently set equal to the blade forces that would exist if the flow were axisymmetric at the local ( $\theta$ ) conditions of the nonaxisymmetric flow. Chima,<sup>34</sup> Hale *et al.*,<sup>35</sup> and Longley<sup>36</sup> use similar modeling approaches, with principal differences being the blade force specification. In Chima’s case, the blade forces are calculated in separate steady-state 3-D Navier-Stokes calculations, whereas in Hale’s case, forces are obtained from axisymmetric throughflow modeling using a streamline curvature method. The present effort is intended for modeling multistage machines, which like the T700 might have order 10 blade rows; therefore, rather than computing the blade forces directly, the body forces are obtained approximately (cf. Longley<sup>36</sup>) at the blade row level by assuming i.) a specified turning schedule which turns the incoming flow to a local blade departure angle based on the blade geometry and the computed short wavelength distortion intensity (aero-blockage); and ii.) the blade force decomposition described in Welch and Larosiliere,<sup>37</sup> which relates the local aero-loading corresponding to the local flow turning to the blade-force components.

The nonaxisymmetric actuator-duct modeling effort represents a work in progress. A preliminary result from an inviscid (Euler) calculation of NASA Rotor 35 is shown in Fig. 12b. The coarse grid used for rotor alone and rotor and stator computations is indicated as well. Upon completion, the model is intended to enable efficient simulation of the dynamics of compressors with nonaxisymmetric flow field. The planned next steps include assessment and validation of the model using known axisymmetric performance data (*e.g.*, NASA stage 35 and CC3 centrifugal compressor) followed by simulation of steady-state and dynamic T700 engine performance in support of the stall control effort.

## CONCLUSIONS

An overview of on-going compressor research at NASA GRC which is intended to address technical challenges for future rotorcraft engines was provided. With particular attention given to the variable rotor requirements of LCTR future applications, the technical challenges for the compressor are associated with low corrected flows in the aft stages, high compressor discharge temperatures, and compressor stability management. The on-going research described includes modeling and experimental efforts that address aerodynamic challenges associated with low corrected flow aft stages and compressor stability. Described modeling efforts are intended to enhance future predictive and assessment capability for multistage compressors, at both the cycle deck and component simulation levels. The T700 testing in the Engine Components Research Laboratory is demonstrating the applicability of stall control approaches in the engine, and related URANS simulations are elucidating the flow physics of stall and its inception. Finally, the three-year NRA contract is underway to develop a state-of-the-art centrifugal compressor stage with advanced aerodynamics which is to be tested in the NASA Small Engine Component Test Facility. The intent is that this new state-of-the-art rotorcraft-relevant compressor stage will serve as a experimental test vehicle for attainment of industry/academia/government consensus data sets needed for code validation and to fill gaps in the knowledge base.

## ACKNOWLEDGMENT

This effort is sponsored by the Subsonic Rotary Wing project of the NASA Fundamental Aeronautics Program. Portions of this work were conducted under the ARL Army Stall Control Engine Demonstrator program, funded through the Army Research Office.

## REFERENCES

- <sup>1</sup>Advanced Affordable Turbine Engine program, Solicitation number W911W60720002, Aviation Applied Technology Directorate, Dec., 2006.
- <sup>2</sup>Johnson, W., Yamauchi, G. K., and Watts, M. E., "NASA Heavy Lift Rotorcraft Systems Investigation," NASA TP-2005-213467, September 2005.
- <sup>3</sup>Acree, C. W., Hyeonsoo, Y., and Sinsay, J. D., "Performance Optimization of the NASA Large Civil Tiltrotor," *Proc. International Powered Lift Conf.*, London, UK, July 22-24, 2008.
- <sup>4</sup>Tenney, B. S., "Joint Heavy Lift (JHL) Overview," *Proc. International Powered Lift Conf.*, London, UK, July 22-24, 2008.
- <sup>5</sup>Snyder, C. A. and Thurman, D. R., "Gas Turbine Characteristics for a Large Civil Tilt-Rotor (LCTR)," *Proc. AHS International, 65th Ann. Forum & Tech. Display*, Grapevine, Texas, May 27-29, 2009.
- <sup>6</sup>Jones, S. M., "An Introduction to Thermodynamic Performance Analysis of Aircraft Gas Turbine Engine Cycles Using the Numerical Propulsion System Simulation Code," NASA/TM-2007-214690, 2007.
- <sup>7</sup>Gauntner, J. W., "Algorithm for Calculating Turbine Cooling Flow and the Resulting Decrease in Turbine Efficiency," NASA TM-81453, 1980.
- <sup>8</sup>Skoch, G. J., Moore, R. D., "Performance of Two 10-lb/sec Centrifugal Compressors With Different Blade and Shroud Thicknesses Operating Over a Range of Reynolds Numbers," AIAA 87-1745, July 1987.
- <sup>9</sup>Larosiliere, L. M., Wood, J. R. and Hathaway M. D., "Aerodynamic Design Study of Advanced Multistage Axial Compressor," NASA TP-2002-211568, Dec., 2002.
- <sup>10</sup>Cumpsty, N. A., *Compressor Aerodynamics*, Krieger, FL, USA, 2004.
- <sup>11</sup>Wisler, D. C., "Loss Reduction in Axial-Flow Compressors through Low-Speed Model Testing," *J. of Eng. Gas Turbines and Power*, Vol. 107, 1985, pp. 354-363.
- <sup>12</sup>Freeman, C., "Effect of Tip Clearance Flow on Compressor Stability and Engine Performance," von Karman Institute for Fluid Dynamics, Lecture series 1985-05, 1985.
- <sup>13</sup>Robbins, W. H. and Dugan, Jr., J. F., "Prediction of Off-Design Performance of Multistage Compressors," NASA SP-36, Chapter 10, 1965, pp. 297-310.
- <sup>14</sup>Smith, L. H., Jr., "The Effect of Tip Clearance on the Peak Pressure rise of Axial Flow Fans and Compressors," ASME Symposium on Stall, 1958, pp. 149-152.
- <sup>15</sup>Koch, C. C. and Smith, L. H., Jr., "Loss Sources and Magnitudes in Axial-Flow Compressors," *J. of Eng. for Power*, Vol 98, 1976, pp. 411-424.
- <sup>16</sup>Brokopp, R. A. and Gronski, R. S., "Small Engine Components Test Facility Compressor Testing Cell," AIAA 92-3980, July, 1992; also NASA TM-105685, 1992.
- <sup>17</sup>Skoch, G. J., Prahst, P. S., Wernet, M. P., Wood, J. R., Strazisar, A. J., "Laser Anemometer Measurements of the Flow Field in a 4:1 Pressure Ratio Centrifugal Impeller," NASA TM-107541, June, 1997.
- <sup>18</sup>Wernet, M. P., Bright, M. M., and Skoch, G. J., "An Investigation of Surge in a High-Speed Centrifugal Compressor Using Digital PIV," *J. Turbomachinery*, Vol. 123, Apr. 2001, pp. 418-218.
- <sup>19</sup>Larosiliere, L. M., Skoch, G. J., Prahst, P. S., "Aerodynamic Synthesis of a Centrifugal Impeller using CFD and Measurements," AIAA-97-2878, July, 1997; also NASA TM-107515 and ARL-TR-1461, July, 1997.
- <sup>20</sup>Adamczyk, J. J., Hansen, J. L., and Prahst, P. S., "A Post Test Analysis of a High-Speed Two-Stage Axial Flow Compressor," ASME GT2007-28057, May, 2007.
- <sup>21</sup>Suder, K. L., Hathaway, M. D., Thorp, S., Strazisar, A. J., Bright, M. M., "Compressor Stability Enhancement Using Discrete Tip Injection," *J. Turbomachinery*, Vol. 123 (1), Jan. 2001, pp. 14-23.
- <sup>22</sup>Strazisar, A. J., Bright, M. M., Thorp, S., Culley, D. E., Suder, K. L., "Compressor Stall Control through Endwall Recirculation," ASME GT2004-54295, June, 2004.
- <sup>23</sup>Skoch, G. J., "Experimental Investigation of Centrifugal Compressor Stabilization Techniques," *J. Turbomachinery*, Vol. 25, Oct. 2003, pp. 704-713.
- <sup>24</sup>Skoch, G. J., "Experimental Investigation of Diffuser Hub Injection to Improve Centrifugal Compressor Stability," *J. Turbomachinery*, Vol. 127, Jan. 2005, pp. 107-117.

- <sup>25</sup>Weigl, H. J., Paduano, J. D., Frechette, L. G., Epstein, A. H., Greitzer, E. M., Bright, M. M., and Strazisar, A. J., "Active Stabilization of Rotating Stall and Surge in a Transonic Single Stage Axial Compressor," *J. Turbomachinery*, Vol. 120. (4), 1998, pp. 625-636.
- <sup>26</sup>Hathaway, M. D., Strazisar, A. J., Impact of Discrete Tip Injection on Stabilization of a Transonic Compressor Rotor," *Proc. 21st Army Science Conference*, Norfolk, Virginia, June 15-17, 1998.
- <sup>27</sup>Hathaway, M. D., Chen, J., Webster, R., G. P. Herrick, "Unsteady Simulation of the Stall Inception Process in the Compression System of a US Army Helicopter Gas Turbine Engine – Final Year Progress," DoD High Performance Computing Modernization Office sponsored "2005 Users Group Conference", Nashville, TN June 27-30, 2005.
- <sup>28</sup>Chen, J.-P., Chen, J.P., Webster, R.S., Hathaway, M.D., Herrick, G.P., and Skoch, G.J., "Numerical Simulation of Stall and Stall Control in Axial and Radial Compressors," AIAA 2006-418, Jan. 2006.
- <sup>29</sup>Chen, J.-P., Hathaway, M. D., Herrick, G. P., "Pre-stall Behavior of a Transonic Axial Compressor Stage via Time Accurate Numerical Simulation," *J. Turbomachinery*, Vol. 130, Oct., 2008, p. 041014.
- <sup>30</sup>Chen, J. P., Johnson, B., Hathaway, M. D., Webster, R. S., "Flow Characteristics of Tip-Injection on Compressor Rotating Spike via Time-Accurate Simulation," (accepted for publication in the 2009 *AIAA J.*).
- <sup>31</sup>Xu, L., Hynes, T.P. and Denton, J.D., "Towards Long Length Scale Unsteady Modelling in Turbomachines", *Proc. IMechE, Pt A: J. Power and Energy*, Vol. 217, 2003.
- <sup>32</sup>Thomas, J. P., Dowell, E. H., and Hall, K. C., "A Harmonic Balance Approach for Modeling Three-Dimensional Nonlinear Unsteady Aerodynamics and Aeroelasticity," IMECE-2002-32532, Nov., 2002.
- <sup>33</sup>Welch, G. E., "Determination of Critical Sector Angle of Inlet Swirl Distortion," AIAA 2007-5057, July, 2007.
- <sup>34</sup>Chima, R. V., "A Three-Dimensional Unsteady CFD Model of Compressor Stability," ASME GT2006-90040, May, 2006.
- <sup>35</sup>Hale, A., and O'Brien, W. O., 1998, "A Three-Dimensional Turbine Engine Analysis Compressor Code (TEACC) For Steady State Inlet Distortion," *J. Turbomachinery*, Vol. 120, pp. 422-430.
- <sup>36</sup>Longley, J. P., "Calculating Stall and Surge Transients," ASME GT2007-27378, May, 2007.
- <sup>37</sup>Welch, G. E. and Larosiliere, L. M., "Passage-Average Description of Wave Rotor Flow," AIAA-97-3144, July, 1997.